Floquet Quantum Criticality

William Berdanier[a,1], **Michael Kolodrubetz**[b,c], **S. A. Parameswaran**[d,2], **and Romain Vasseur**[e]

[a]Department of Physics, University of California, Berkeley, CA 94720, USA; [b]Materials Sciences Division, Lawrence Berkeley National Laboratory, Berkeley, CA 94720, USA; [c]Department of Physics, The University of Texas at Dallas, Richardson, Texas 75080, USA; [d]The Rudolf Peierls Centre for Theoretical Physics, University of Oxford, Oxford OX1 3NP, UK; [e]Department of Physics, University of Massachusetts, Amherst, Massachusetts 01003, USA

This manuscript was compiled on July 6, 2018

We study transitions between distinct phases of one-dimensional periodically driven (Floquet) systems. We argue that these are generically controlled by infinite-randomness fixed points of a strong-disorder renormalization group procedure. Working in the fermionic representation of the prototypical Floquet Ising chain, we leverage infinite randomness physics to provide a simple description of Floquet (multi)criticality in terms of a new type of domain wall associated with time-translational symmetry-breaking and the formation of 'Floquet time crystals'. We validate our analysis via numerical simulations of free-fermion models sufficient to capture the critical physics.

quantum criticality | disordered systems | many-body localization | periodically driven systems | non-perturbative arguments

The assignment of robust phase structure to periodically driven quantum many-body systems is among the most striking results in the study of non-equilibrium dynamics (1). There has been dramatic progress in understanding such 'Floquet' systems, ranging from proposals to engineer new states of matter via the drive (2–12) to the classification of driven analogs of symmetry-protected topological phases ('Floquet SPTs') (13–20). These typically require that the system under investigation possess one or more microscopic global symmetries. In addition, *all* Floquet systems share an invariance under time translations by an integer multiple of their drive period. Unlike the continuous time translational symmetry characteristic of undriven Hamiltonian systems (21–23), this discrete symmetry may be spontaneously broken, leading to a distinctive dynamical response at rational fractions of the drive period — a phenomenon dubbed 'time crystallinity' (24–29). The time translation symmetry breaking (TTSB) exhibited by Floquet time crystals is stable against perturbations that preserve the periodicity of the drive, permitting generalizations of notions such as broken symmetry and phase rigidity to the temporal setting. Experiments have begun to probe these predictions in well-isolated systems such as ultracold gases, ion traps (30), nitrogen-vacancy centers in diamond (31), and even spatially ordered crystals (32, 33).

In light of these developments, it is desirable to construct a theory of Floquet (multi-)critical points between distinct Floquet phases. Ideally, this should emerge as the fixed point of a coarse-graining/renormalization group procedure, enable us to identify critical degrees of freedom, especially those responsible for TTSB, and allow us to compute the critical scaling behavior.

Here, we develop such a theory for a prototypical Floquet system: the driven random quantum Ising chain. Extensive analysis has shown that this model hosts four phases (1, 24). Two of these, the paramagnet (PM) and the spin glass (SG), are present already in the static problem (34–36). A third, the π spin glass/time crystal, has spatiotemporal long-range order and subharmonic bulk response at half-integer multiples of the drive frequency. This phase, and its Ising dual — the 0π paramagnet, which also exhibits TTSB but only at the boundaries of a finite sample — are unique to the driven setting. A precise understanding of the (multi)critical points between these distinct Floquet phases accessed by tuning drive parameters is the subject of this work.

Our approach relies on the presence of quenched disorder, required for a generic periodically-driven system to have Floquet phase structure rather than thermalize to a featureless infinite-temperature state (37–40). We argue that transitions between distinct one-dimensional Floquet phases are then best described in terms of an infinite-randomness fixed point accessed via a strong-disorder real space renormalization group procedure. In the non-equilibrium setting, the stability of infinite-randomness fixed points against thermalization via long-range resonances remains a topic of debate (41–43). However, even if unstable, we expect that they will control the dynamics of prethermalization relevant to all reasonably accessible experimental timescales (44, 45).

The universality of our analysis turns on the fact that, in the vicinity of such infinite-randomness critical points, a typical configuration of the system can be viewed as being composed of domains deep in one of two proximate phases (46–51). Transitions that do *not* involve TTSB (i.e., the SG/PM or 0πPM/πSG transitions) map to the static (random) Ising critical point and can be understood in similar terms. In contrast, transitions that involve the onset of TTSB in the bulk (PM to πSG) or at the boundary (SG to 0πPM) can be understood in terms of a new class of domain wall special to

Significance Statement

Periodically driven "Floquet" systems are non-equilibrium systems whose time-translation symmetry can give rise to a rich dynamical phase structure. In the presence of quenched disorder, they can avoid thermalizing to a bland infinite temperature state through a phenomenon known as many-body localization (MBL). The ability of these driven MBL phases to host phenomena forbidden in equilibrium, such as "time crystallinity," has gained widespread interest in recent years. In this work, we consider the question of criticality that emerges at the transitions between distinct Floquet MBL phases. By providing a universally applicable picture and applying it to a prototypical driven system, the driven Ising chain, we identify new critical points and give an understanding of Floquet criticality in general.

All authors contributed to the design of the research and the theoretical analysis of the data and in writing the paper.

The authors declare no conflict of interest.

[1]To whom correspondence should be addressed. E-mail: wberdanier@berkeley.edu.
[2] On leave from: Department of Physics and Astronomy, University of California Irvine, Irvine, CA 92697, USA.

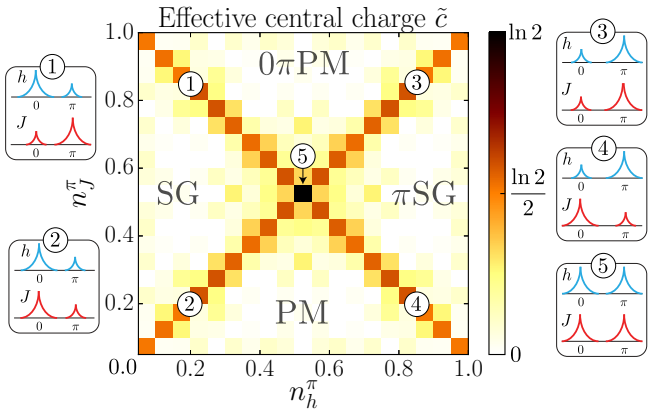

Fig. 1. Phase diagram deduced by fitting "effective central charge" from entanglement scaling (see Fig. 3 for details). Insets: sketches of infinite-randomness coupling distributions along the critical lines (1-4) and at the multicritical point (5).

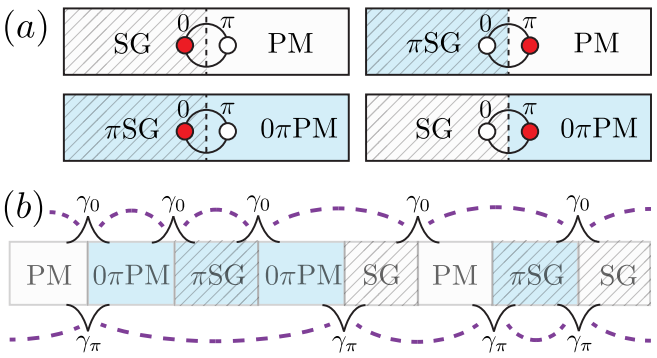

Fig. 2. (a) Domain walls (DWs) between proximate phases of the driven Ising model. In fermionic language, these host topological edge states at either 0 or π quasienergy (red). Blue regions exhibit bulk/boundary time-translational symmetry breaking (TTSB), and hatched regions have bulk spin glass order. (b) A typical multicritical configuration. Tunneling between DW states $\gamma_{0,\pi}$ yields two independent chains around 0 and π quasienergy.

driven systems, that separate regions driven at a frequency primarily near 0 or near π — a picture we verify numerically. When the Ising model is rewritten as a fermion problem, this picture yields a simple description of Floquet criticality in terms of domain walls that bind Majorana states at quasienergy 0 or π, allowing us to further study the multicritical point where all four phases meet.

Model. Floquet systems are defined by a time-periodic Hamiltonian $H(t) = H(t+T)$. For reasons similar to Bloch's theorem, eigenstates satisfy $\big|\psi_\alpha(t)\big\rangle = e^{-iE_\alpha t}\big|\phi_\alpha(t)\big\rangle$, where $\big|\phi_\alpha(t+T)\big\rangle = \big|\phi_\alpha(t)\big\rangle$ and we set $\hbar = 1$ (52, 53). In contrast to the case of static Hamiltonians, the quasi-energies E_α are only defined modulo $2\pi/T$, voiding the notion of a 'ground state'.

An object of fundamental interest is the single-period evolution operator or Floquet operator $F \equiv U(T)$. If disorder is strong enough, F can have an extensive set of local conserved quantities. This implies area-law scaling of entanglement in Floquet eigenstates, and consequently the absence of thermalization (54).

Unlike generic (thermalizing) Floquet systems, such many-body localized (MBL) Floquet systems retain a notion of phase structure to infinitely long times. For concreteness, we focus on the driven quantum Ising chain, the simplest Floquet system that hosts uniquely dynamical phases. The corresponding Floquet operator is

$$F = \mathrm{e}^{-i\frac{T}{2}\sum_i J_i\sigma_i^z\sigma_{i+1}^z + U\sigma_i^z\sigma_{i+2}^z}\mathrm{e}^{-i\frac{T}{2}\sum_i h_i\sigma_i^x + U\sigma_i^x\sigma_{i+1}^x}, \quad [1]$$

where σ_i^α are Pauli operators. Here J_i and h_i are uncorrelated random variables, and U corresponds to small interaction terms that respect the $\mathbb{Z}_2$ symmetry of the model generated by $G_{\mathrm{Ising}} = \prod_i \sigma_i^x$. For specificity, we draw couplings h, J randomly with probability $n_\pi^{h,J}$ from a box distribution of maximal width about π, namely $[\pi/2, 3\pi/2]$, and with probability $n_0^{h,J} = 1 - n_\pi^{h,J}$ from a box distribution of maximal width about 0, namely $[-\pi/2, \pi/2]$. The reasons for this parametrization will become evident below. F corresponds to an interacting transverse-field Ising model where for $U = 0$ we stroboscopically alternate between field and bond terms. It is helpful to perform a Jordan-Wigner transformation to map bond and field terms to Majorana fermion hopping terms, yielding a p-wave free fermion superconductor with density-density interactions given by U. In the high-frequency limit $T \to 0$, we can rewrite $F = e^{-iH_F T}$ by expanding and re-exponentiating order-by order in T and the Floquet Hamiltonian H_F recovers a static Ising model. We work far from this limit, setting $T = 1$.

Phases and Duality. Observe that $(n_\pi^h, n_\pi^J) = \frac{1}{\pi}(\overline{h_i}, \overline{J_i})$, where the bars denote disorder averages, and hence tune between phases of model Eq. (1) analogously to h, J in the clean case. The four phases are summarized in the phase diagram in Figure 1. The trivial Floquet paramagnet (PM) breaks no symmetries and has short range spin-spin correlations. The spin glass (SG) spontaneously breaks Ising symmetry with long-range spin correlations in time, or equivalently localized edge modes at 0 quasienergy in the fermion language. These two phases are connected to the undriven paramagnet and ferromagnet/spin glass phases of the random Ising model (34–36). Unique to the Floquet system are the π-spin glass (πSG) and the 0π paramagnet (0πPM). The πSG spontaneously breaks both Ising and time translation symmetry in the bulk. Often referred to as a "time crystal" (1, 25, 27), it maps to a fermion phase with localized Majorana edge modes at π quasienergy (55). Finally, the 0πPM has short range bulk correlations but also boundary TTSB; its fermion dual has both 0 and π Majorana edge modes and is a simple example of a Floquet SPT. In the fermion language, domain walls between these different phases host either 0 or π Majorana bound states (Fig. 2a) central to the infinite-randomness criticality discussed below.

The absence of energy conservation in the Floquet setting admits two new eigenstate-preserving changes of parameter to Eq. (1). The transformations $J_j \mapsto J_j + \pi$ and $h_j \mapsto h_j + \pi$ both separately map F onto another interacting Ising-like Floquet operator with precisely the same eigenstates (56), but possibly distinct quasienergies: $J_j \mapsto J_j + \pi$ preserves F exactly (up to boundary terms), while $h_j \mapsto h_j + \pi$ sends $F \mapsto FG_{\mathrm{Ising}} = G_{\mathrm{Ising}}F$. Note that, despite not changing bulk properties of the eigenstates, these transformations map the PM to the 0πPM and the SG to the πSG respectively. Additionally, a global rotation about the y axis takes $h_j \mapsto -h_j$. Below, we fix phase transition lines by combining these *Floquet symmetries* with the usual Ising bond-field duality

that exchanges h and J (and hence SG and PM in the static random case).

Infinite-randomness structure. In analogy with the critical point between PM and SG phases in the static random Ising model (both at zero temperature and in highly excited states), we expect that the dynamical Floquet transitions of Eq. (1) are controlled by an infinite-randomness fixed point (IRFP) of a real space renormalization group (RSRG) procedure. At a static IRFP, the distribution of the effective couplings broadens without bound under renormalization, so the effective disorder strength diverges with the RG scale. A typical configuration of the system in the vicinity of such a transition can be viewed as being composed of puddles deep in one of the two proximate phases, in contrast with continuous phase transitions in clean systems (50, 51).

In order to generalize this picture to the Floquet Ising setting we must identify appropriate scaling variables. For $J_i, h_i \ll \pi$ we recover the criticality of the static model controlled by an IRFP if J_i and h_i are drawn from the same distribution. In this case, the relevant operator at the critical point controls the asymmetry between the J_i, h_i distributions. At static IRFPs, critical couplings are power-law distributed near 0. The absence of energy conservation in the Floquet setting complicates this picture since there is no longer a clear notion of 'low' energies. However, a natural resolution is to allow for fixed-point couplings to be symmetrically and power-law distributed around *both* $0, \pi$ quasienergy (or more generally, all quasienergies that can be mapped to 0 by applying Floquet symmetries of the drive). This introduces a new parameter for Floquet-Ising IRFPs, namely the fractions n_0 and n_π of couplings near 0 and π, respectively. Evidently, we have $n_0 = 1 - n_\pi$. We will show that there is a new type of IRFP specific to the Floquet setting for $n_\pi = 1/2$, where the criticality is tuned by the asymmetry between the distributions at 0 and π quasienergy, at *fixed* values of the J_i - h_i distribution asymmetry.

Emergent π-criticality. For J_i, h_i near 0 ($n_\pi \ll 1$), the IRFP distribution is similar to the static case, and the critical point can be understood in terms of domain walls (DWs) between regions where $J_i \gg h_i$ and those where $J_i \ll h_i$. Standard results show that in the fermionic language each DW binds a Majorana state $\tilde{\gamma}_i^0$ at zero quasienergy, and the transition can be understood in terms of these. For $n_\pi \sim 1$, we again have a single IRFP distribution, but now centered at π. However, following (1) we may factor a global π pulse from both terms of the drive, to recover the previous DW structure. Although still at zero quasienergy, here the DW Majoranas drive a transition between πSG-0πPM, owing to the global π-pulse. Again, the relevant parameter tuning the transition is the asymmetry between the distributions of J_i and h_i so the physics is essentially the same.

Quite different physics arises for $n_\pi \sim 1/2$ where the couplings exhibit strong quenched spatial fluctuations between 0 and π. This follows from the fact that there are *distinct* IRFP distributions for couplings near 0 and π, such that the relevant critical physics is captured by a new class of "0π-DWs" unique to the Floquet setting. If J_i is small and $h_i \sim \pi$ (consistent with $n_\pi \sim 1/2$), these correspond to DWs between πSG and PM regions, whereas if h_i is small and $J_i \sim \pi$, the critical behavior can be understood in terms of DWs between SG and 0πPM. In the fermion language each such 0π DW traps a Majorana bound state $\tilde{\gamma}_i^\pi$ at quasienergy π. This may also be deduced by comparing the edge modes of the adjacent phases (Fig. 2a). Since they are topological edge modes, a given π-Majorana trapped at a 0π DW can only couple to other π-Majoranas bound to 0π DWs, leading to a second emergent Majorana fermion chain whose dynamics are independent from the initial chain (Fig. 2b). If the intervening puddles are MBL, the tunneling between π-Majoranas is exponentially suppressed as $\sim \mathrm{e}^{-\ell}$, with the size ℓ of the puddles. Even if we start from a configuration where J and h are drawn from the same distribution, there are still π-Majoranas bound to DWs separating infinite-randomness quantum critical regions where the couplings are near 0 or π (56), and the typical tunnel coupling is stretched exponential $\sim \mathrm{e}^{-\sqrt{\ell}}$ (46, 48). Thus, the tunneling terms between the π-Majoranas remain short-ranged. Crucially, the criticality of this emergent π-Majorana chain is tuned by n_π (with $n_\pi = \frac{1}{2}$ at criticality), independently of the field-bond asymmetry that tunes the usual Ising transition. We emphasize that although the universality class of this transition is still random Ising, it is described by flow towards an IRFP at π quasienergy, and hence the spectral properties of the transition are distinct.

Observe that the PM-πSG transition involves the onset of TTSB, since the πSG is the prototypical example of a time crystal. Similarly, the SG-0πPM transition involves the onset of TTSB at the ends of an open system. Therefore, we identify the 0π DWs as the degrees of freedom that are responsible for changes in TTSB.

RG treatment. The above infinite randomness hypothesis suggests that the critical behavior at the dynamical Floquet transitions can be understood in terms of two effectively static Majorana chains, one near quasienergy 0 ($\tilde{\gamma}_i^0$) and the other near quasienergy π ($\tilde{\gamma}_i^\pi$). While the criticality of the 0 chain is driven by the asymmetry between J and h as in the usual Ising chain, the π chain is critical for $n_\pi = \frac{1}{2}$ where there is a symmetry between 0 and π couplings. This picture can be confirmed explicitly (56) by considering instead the criticality of F^2, which should have couplings only near 0 and is described by an effectively static Hamiltonian $F^2 = \mathrm{e}^{-i2H_F}$. The dynamical properties of these two Majorana chains can be analyzed using standard RG techniques designed for static MBL Hamiltonians (35, 36, 57). We decimate stronger couplings before weaker ones, putting the pair of Majoranas involved in the strongest coupling in a local eigenstate. Iterating this process leads to an IRFP which self-consistently justifies the strong disorder perturbative treatment. The resulting RG equations match those for the static random Ising model, except crucially, we can now have renormalization towards 0 or towards π quasienergies in F reflecting the decoupling of the two effective Majorana chains. This effective decoupling also persists in the presence of interactions ($U \neq 0$). Interactions within the 0 and π Ising chains flow towards 0 under RG much faster than the other couplings and are therefore irrelevant (35, 47). While interactions also permit Floquet-umklapp terms $\tilde{\gamma}_i^0 \tilde{\gamma}_j^0 \tilde{\gamma}_k^\pi \tilde{\gamma}_l^\pi$ that would couple the critical 0 and π chains at the multicritical point, such terms are also irrelevant, and so can be ignored as long as interactions are relatively weak (47, 58–60). While weak interactions are irrelevant at the multicritical point, and very strong interactions are likely to drive thermalization, we leave open the possibility that intermediate interactions might drive the system to a new infinite-randomness critical point in

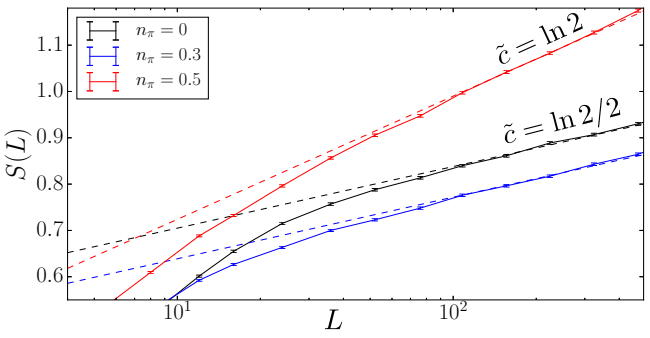

Fig. 3. Scaling with system size of disorder- and eigenstate-averaged entanglement entropy S for a cut at $L/2$. Dashed lines show predicted slopes for strong-disorder Ising criticality along the transition lines (blue, black); this doubles at the multicritical point (red).

the universality class of the random Ashkin-Teller model (59).

Therefore, for sufficiently weak interactions, the critical lines are always in the random Ising universality class. The four-phase multicritical point — at which all four distributions are symmetric — is in the Ising × Ising universality class. This picture of Floquet (multi) criticality extends both symmetry-based reasoning used when all h_i couplings are near π (27), and the analysis of the essentially static $J_i, h_i \ll 1$ (61) case.

Floquet (multi)criticality. Combining this reasoning with standard IRFP results, we conclude that all the transitions show infinite-randomness Ising scaling: the correlation length diverges as $\xi \sim |\Delta|^{-\nu}$ where Δ characterizes the deviation from the critical lines, and $\nu = 2$ or 1 for average or typical quantities, respectively (46, 48). This scaling should have universal signatures in dynamical (or eigenstate) correlation functions (27, 35, 46, 48), and in particular in the eigenstate entanglement entropy (57, 62, 63). Assuming a system of size L and open boundary conditions, the half-system entanglement entropy should scale with system size as $S_L \sim (\tilde{c}/6)\ln L$, up to nonuniversal additive contributions, with "effective central charge" $\tilde{c} = \ln 2/2$ (62). At the multicritical point, we predict $\tilde{c} = \ln 2$ due to the criticality of the 0 and π Majorana chains. Our picture also predicts an emergent $\mathbb{Z}_2 \times \mathbb{Z}_2$ symmetry at the multicritical point, where the additional $\mathbb{Z}_2$ symmetry can be constructed explicitly as $D = F\sqrt{F^2}^\dagger$ (24, 26, 27). For a multicritical configuration with couplings near 0 or π, we find that D is distinct from the original Ising symmetry of the model, and coincides with the fermion parity of the emergent π-Majorana chain,

$$D = \prod_{j\in\{0\pi\ \mathrm{DWs}\}} \tilde{\gamma}_j^\pi . \qquad [2]$$

Numerics. As stressed above, our picture of these transitions relies on the infinite randomness assumption. To justify this and to confirm our analytical predictions, we have performed extensive numerical simulations on the non-interacting model, leveraging its free-fermion representation to access the full single-particle spectrum and to calculate the entanglement entropy of arbitrary eigenstates (56). We average over 20,000 disorder realizations (with open boundary conditions), randomly choosing a Floquet eigenstate in each.

Given our parametrization of disorder, the combination $\frac{1}{2}(n_\pi^h - n_\pi^J)$ provides a measure of the asymmetry between J and h couplings, while $\frac{1}{2}(n_\pi^h + n_\pi^J)$ measures the average probability of a π coupling. Therefore, from our reasoning above and using the usual Ising duality, we expect a critical line for $n_J^\pi = n_h^\pi$. Combining the Ising duality with Floquet symmetries leads to another critical line $n_J^\pi + n_h^\pi = 1$ where we expect 0π infinite randomness behavior. Note that the bare disorder distributions are far from the infinite randomness fixed point expected to emerge at criticality. Nonetheless, as shown in Figure 3, we observe clear logarithmic scaling of entanglement along the self-dual lines $n_J^\pi = n_h^\pi$ and $n_J^\pi + n_h^\pi = 1$ of Eq. Eq. (1). We find $\tilde{c} \approx \ln 2/2$, consistent with the prediction that the lines are in the random Ising universality class. Deep in the phases, we find $\tilde{c} \approx 0$ consistent with the area-law scaling expected for Floquet MBL phases (64, 65). At the multicritical point $n_\pi^h = n_\pi^J = 1/2$, we find $\tilde{c} \approx \ln 2$, consistent with our expectation of two decoupled critical Ising chains. Although stability to quartic interchain couplings cannot be addressed in this noninteracting limit, we expect it on general grounds (47, 58, 59), modulo usual caveats on thermalization. Fig. 1, showing the entanglement scaling across the entire phase diagram, summarizes these results. Finally, we have also numerically calculated the relative number of single particle quasienergies near 0 and near π, finding good agreement with a simple prediction from the infinite-randomness domain wall picture (56). Moreover, Fig. 1 clearly shows that changing $n_J^\pi \pm n_h^\pi$ tunes across the critical lines, confirming that these parameters control distribution asymmetries as in the IRFP picture (Fig. 1, insets).

Experimental consequences. Let us now turn to some experimental consequences of the above predictions. Recent advances in the control of ultracold atomic arrays have brought models such as Eq. 1 into the realm of experimental realizability (66–68). The model hosts a time-crystal phase (the π spin glass), the phenomenology of which has recently been directly observed (30, 31). Even though, as mentioned earlier, these critical lines may eventually thermalize due to long-range resonances (41–43), the dynamics of the Ising universality class should persist through a prethermalization regime relevant to all reasonably accessible experimental timescales (44, 45). Thus, the dynamical signatures of the transitions we have identified should be readily experimentally observable.

One prominent experimental signature of this physics is the scaling behavior of the dynamical spin-spin autocorrelation function in Fourier space $C(\omega, t) \equiv \int_0^\infty d\tau e^{-i\omega\tau}\overline{\langle\sigma_i^z(t+\tau)\sigma_i^z(\tau)\rangle}$, with the overline representing a disorder average (27). In accordance with the random Ising universality class, the spin-spin autocorrelation function will scale as $\overline{\langle\sigma_i^z(t)\sigma_i^z(0)\rangle} \sim 1/\log^{2-\phi} t$ (35), with the overline representing a disorder average and $\phi = (1+\sqrt{5})/2$ the golden ratio. Performing the Fourier transform, our analysis then predicts that along the $n_h^\pi = n_J^\pi$ critical line of the model, the Fourier peak at 0 quasienergy will decay as $C(0,t) \sim 1/\log^{2-\phi} t$; along the $n_h^\pi = 1 - n_J^\pi$ critical line the peak at π quasienergy will decay the same way as $C(\omega/2, t) \sim 1/\log^{2-\phi} t$; and at the multicritical point, both peaks will decay in this way simultaneously, giving

$$C(0,t) \sim C(\omega/2, t) \sim \frac{1}{\log^{2-\phi} t}. \qquad [3]$$

This slow, logarithmic decay, independently for the decoupled chains at 0 and $\omega/2$, serves as an unambiguous signature of the

universal multicritical physics we describe. The fact that the two decays are independent is highly nontrivial, since generic $\mathbb{Z}_2 \times \mathbb{Z}_2$ multicritical points would have distinct scaling from either $\mathbb{Z}_2$ individually.

Discussion. We have presented a generic picture of the transitions between MBL Floquet phases, and applied it to study the criticality of the periodically driven interacting random Ising chain. Our work can be generalized to more intricate Floquet systems, under the (reasonable) assumption that they flow to infinite randomness under coarse-graning. The resulting IRFP is enriched in the Floquet setting: each distinct invariant Floquet quasienergy hosts an independent set of fixed-point coupling distributions. (For instance the $\mathbb{Z}_n$ model has n such invariant quasienergies, $2\pi k/n$, with $k = 1, \ldots, n$.) Systems at conventional IRFPs are tuned across criticality by adjusting the imbalance between distributions of distinct couplings at the *same* quasienergy. At Floquet IRFPs, we may hold such single-quasienergy imbalances fixed and instead tune the imbalance between the distributions of couplings at *distinct* quasienergies. Transitions driven by such cross-quasienergy imbalances will usually involve an onset or change of TTSB in the bulk or at the boundary, and in this sense describe "time crystallization". In some cases, it may be possible to leverage a Jordan-Wigner mapping in conjunction with these infinite-randomness arguments to arrive at a domain-wall description of the critical/multicritical physics. We anticipate that a variety of Floquet symmetry-breaking/symmetry-protected topological phases will be amenable to similar analysis, but we defer an exhaustive study to future work.

Materials and Methods

Numerical simulations were performed on the transverse-field Ising (TFI) chain, where we extract the entanglement entropy across a cut of length l from the boundary in an arbitrary eigenstate. We utilize the fact that the non-interacting TFI chain can be efficiently described as a system of free Majorana fermions (69, 70), details of which follow.

First, let us apply a Jordan-Wigner transformation to the TFI chain $\sigma_j^x = i\gamma_{2j}\gamma_{2j+1}$, $\sigma_j^y = \left(\prod_{l<j} i\gamma_{2l}\gamma_{2l+1}\right)\gamma_{2j+1}$, $\sigma_j^z = \left(\prod_{l<j} i\gamma_{2l}\gamma_{2l+1}\right)\gamma_{2j}$, where the γ operators obey the Majorana algebra $\{\gamma_i, \gamma_j\} = 2\delta_{ij}$, $\gamma_i^2 = 1$, $\gamma_i^\dagger = \gamma_i$. This implies that $\sigma_j^z\sigma_{j+1}^z = i\gamma_{2j+1}\gamma_{2j+2}$. In the Majorana language, our periodically driven TFI Hamiltonian is

$$H(t) = \begin{cases} H_1 = i\sum_{j=0}^{L-1} h_j\gamma_{2j}\gamma_{2j+1} & 0 \le t \le T_1 \\ H_2 = i\sum_{j=0}^{L-2} J_j\gamma_{2j+1}\gamma_{2j+2} & T_1 \le t \le T_1 + T_2 = T \end{cases} \quad [4]$$

where we set $T_1 = T_2 = 1/2$ for convenience. Now, if we are in a state satisfying Wick's theorem, the density matrix and all derived quantities are determined by the two-point correlator $C_{ij} = \langle\gamma_i\gamma_j\rangle$. The Majorana anti-commutation relation implies that $C_{ij} = 2\delta_{ij} - C_{ji}$, so $C_{ij} = \delta_{ij} + a_{ij}$, where a is some antisymmetric matrix.

Let us first construct the Floquet evolution operator. To see how a Hamiltonian evolves the correlation function, first note that in the Heisenberg picture $C_{ij}(t) = \langle\gamma_i(t)\gamma_j(t)\rangle$. For A and B (distinct) Majorana operators, we have $e^{\alpha AB} = \cos\alpha + AB\sin\alpha$. Thus, $e^{\alpha AB}Ae^{-\alpha AB} = A\cos 2\alpha - B\sin 2\alpha$, and $e^{\alpha AB}Be^{-\alpha AB} = B\cos 2\alpha + A\sin 2\alpha$. If our Hamiltonian were not already in block-diagonal form, we would first need to pseudo-diagonalize it (in this case, perform a Schur decomposition) into the form $Q^THQ = \sum_i \epsilon_i\gamma'_{2i}\gamma'_{2i+1}$, where $\gamma'_i = Q_{ij}\gamma_j$. Then, defining the block-diagonal matrix

$$D(t) = \mathrm{diag}\left[\begin{pmatrix}\cos(2\epsilon_k t) & -\sin(2\epsilon_k t)\\ \sin(2\epsilon_k t) & \cos(2\epsilon_k t)\end{pmatrix}\right]_{k=1}^{2L} \quad [5]$$

we find that $\gamma'_i(t) = D_{ij}(t)\gamma'_j(0)$. Defining $\Gamma(t) \equiv Q^TD(t)Q$, we see that the correlation function evolves simply as $C(t) = \Gamma(t)C(0)\Gamma(t)^T$. To construct the Floquet evolution operator, then, we write

$$F = U(T) = e^{-iT_2H_2}e^{-iT_1H_1} = Q_2^TD_2(T_2)Q_2Q_1^TD_1(T_1)Q_1. \quad [6]$$

For the simple drive considered above, H_1 and H_2 are already block-diagonal, so their Q matrices are trivial and the exponentiation to construct each time evolution can be done explicitly. However, we do now need to perform a Schur decomposition on F to bring it into block-diagonal form, given by a real orthogonal matrix Q_F. This rotates to the basis of single-particle Floquet eigenstates, with λ_F^i the single-particle quasi-energies.

The initial correlation function is simple in this basis: it will also be block diagonal with blocks of $\pm\sigma_x$, where the positive sign occupies the mode and the negative sign leaves it empty. Therefore, for an arbitrary Floquet eigenstate in the diagonal basis, $C' = \mathrm{diag}(\pm\sigma_x)_{i=1}^L$. We can then rotate back to the original variables by $C = Q_FC'Q_F^T$.

Note that the 0 and π modes that emerge from our RSRG picture show up numerically as nearly degenerate states whose quasienergies must be resolved. In practice, this required implementing high-precision numerics – beyond conventional machine precision – which is described in more detail in the appendix (56).

The above steps allow us to access the correlation function in any Floquet eigenstate. Let us now show how to calculate the entanglement entropy from that C matrix. First, diagonalize the antisymmetric part of the correlation function $a = q^T\sigma q$, where q is orthogonal and σ has form $\sigma = \mathrm{diag}\begin{pmatrix}0 & \lambda_i\\ -\lambda_i & 0\end{pmatrix}_{i=1}^L$. This can be achieved by a Schur decomposition, where the pseudo-eigenvalues are arranged such that $\sigma_{i,i+1} = \lambda_i$, and $\sigma^T = -\sigma$. Now define $\gamma' = q\gamma$. Then

$$\left\langle\gamma'_{2k'-1}\gamma'_{2k}\right\rangle = q_{2k'-1,i}q_{2k,j}(\delta_{ij} + \lambda_{k''}(q_{2k''-1,i}q_{2k'',j} - q_{2k'',i}q_{2k''-1,j})). \quad [7]$$

From the orthogonality of q, $q_{\alpha i}q_{\beta i} = \delta_{\alpha\beta}$, so the only non-vanishing term is $q_{2k'-1,i}q_{2k,j}\lambda_{k''}q_{2k''-1,i}q_{2k'',j} = \lambda_k\delta_{kk'}\delta_{k'k''}$. Thus the only non-vanishing two-point function is

$$\left\langle\gamma'_{2k-1}\gamma'_{2k}\right\rangle = -\left\langle\gamma'_{2k}\gamma'_{2k-1}\right\rangle = \lambda_k. \quad [8]$$

We can write this correlation function as arising from a single particle density matrix $\rho = \frac{1}{Z}\prod_k e^{i\epsilon_k\gamma'_{2k-1}\gamma'_{2k}}$. Now, we can construct complex fermion operators from Majorana operators via $c_k = \frac{\gamma'_{2k-1}+i\gamma'_{2k}}{2}$, $c_k^\dagger = \frac{\gamma'_{2k-1}-i\gamma'_{2k}}{2}$, so $\gamma'_{2k-1}\gamma'_{2k} = -i(2c_k^\dagger c_k - 1)$. This gives the density matrix as

$$\rho = \prod_k \frac{e^{\epsilon_k(2c_k^\dagger c_k - 1)}}{e^{\epsilon_k} + e^{-\epsilon_k}}.$$

Thus the two-point function is $\left\langle\gamma'_{2k-1}\gamma'_{2k}\right\rangle = -i\left\langle 2c_k^\dagger c_k - 1\right\rangle = \lambda_k = -i\frac{e^{\epsilon_k} - e^{-\epsilon_k}}{e^{\epsilon_k} + e^{-\epsilon_k}} = -i\tanh\epsilon_k$. Now define $\mu_k = |\lambda_k|$, giving $\epsilon_k = \tanh^{-1}(\mu_k)$. To find the entanglement entropy, write the density matrix as

$$\rho = \prod_k \left[p_k\left|0_k\right\rangle\left\langle 0_k\right| + (1-p_k)\left|1_k\right\rangle\left\langle 1_k\right|\right], \quad p_k = \frac{e^{-\epsilon_k}}{e^{\epsilon_k} + e^{-\epsilon_k}}. \quad [9]$$

Then the entanglement entropy in an arbitrary Floquet eigenstate is $S = -\mathrm{Tr}\rho\log\rho = -\sum_{k=1}^L p_k\log p_k + (1-p_k)\log(1-p_k)$.

ACKNOWLEDGMENTS. We thank Vedika Khemani, Shivaji Sondhi, Dominic Else, Chetan Nayak, Adam Nahum, Joel Moore, David Huse and especially Shtitadhi Roy for useful discussions, and

are grateful to David Huse and Vedika Khemani for detailed comments on the manuscript. This work used the Extreme Science and Engineering Discovery Environment (XSEDE)(71), which is supported by National Science Foundation grant number ACI-1053575. W.B. acknowledges support from the Department of Defense (DoD) through the National Defense Science & Engineering Graduate Fellowship (NDSEG) Program, and from the Hellman Foundation through a Hellman Graduate Fellowship. We also acknowledge support from Laboratory Directed Research and Development (LDRD) funding from Lawrence Berkeley National Laboratory, provided by the Director, Office of Science, of the U.S. Department of Energy under Contract No. DEAC02-05CH11231, and the DoE Basic Energy Sciences (BES) TIMES initiative (M.K.); travel support from the California Institute for Quantum Emulation (CAIQUE) via PRCA award CA-15- 327861 and the California NanoSystems Institute at the University of California, Santa Barbara (W.B. and S.A.P.); support from NSF Grant DMR-1455366 at the University of California, Irvine (S.A.P.); and University of Massachusetts start-up funds (R.V.).

1. Khemani V, Lazarides A, Moessner R, Sondhi SL (2016) Phase structure of driven quantum systems. Phys. Rev. Lett. 116(25):250401.
2. Eckardt A (2017) Colloquium. Rev. Mod. Phys. 89(1):011004.
3. Bukov M, D'Alessio L, Polkovnikov A (2015) Universal high-frequency behavior of periodically driven systems: from dynamical stabilization to floquet engineering. Advances in Physics 64(2):139–226.
4. Meinert F, Mark MJ, Lauber K, Daley AJ, Nägerl HC (2016) Floquet engineering of correlated tunneling in the bose-hubbard model with ultracold atoms. Phys. Rev. Lett. 116(20):205301.
5. Holthaus M (2016) Floquet engineering with quasienergy bands of periodically driven optical lattices. Journal of Physics B: Atomic, Molecular and Optical Physics 49(1):013001.
6. Goldman N, Dalibard J (2014) Periodically driven quantum systems: Effective hamiltonians and engineered gauge fields. Phys. Rev. X 4(3):031027.
7. Kitagawa T, Berg E, Rudner M, Demler E (2010) Topological characterization of periodically driven quantum systems. Phys. Rev. B 82(23):235114.
8. Lindner NH, Refael G, Galitski V (2011) Floquet topological insulator in semiconductor quantum wells. Nature Physics 7:490 EP –.
9. Rudner MS, Lindner NH, Berg E, Levin M (2013) Anomalous edge states and the bulk-edge correspondence for periodically driven two-dimensional systems. Phys. Rev. X 3(3):031005.
10. Nathan F, Rudner MS (2015) Topological singularities and the general classification of floquet–bloch systems. New Journal of Physics 17(12):125014.
11. Oka T, Aoki H (2009) Photovoltaic hall effect in graphene. Phys. Rev. B 79(8):081406.
12. Görg F, et al. (2018) Enhancement and sign change of magnetic correlations in a driven quantum many-body system. Nature 553:481 EP –.
13. Iadecola T, Santos LH, Chamon C (2015) Stroboscopic symmetry-protected topological phases. Phys. Rev. B 92(12):125107.
14. von Keyserlingk CW, Sondhi SL (2016) Phase structure of one-dimensional interacting floquet systems. i. abelian symmetry-protected topological phases. Phys. Rev. B 93(24):245145.
15. von Keyserlingk CW, Sondhi SL (2016) Phase structure of one-dimensional interacting floquet systems. ii. symmetry-broken phases. Phys. Rev. B 93(24):245146.
16. Else DV, Nayak C (2016) Classification of topological phases in periodically driven interacting systems. Phys. Rev. B 93(20):201103.
17. Potter AC, Morimoto T, Vishwanath A (2016) Classification of Interacting Topological Floquet Phases in One Dimension. Phys. Rev. X 6(4):041001.
18. Roy R, Harper F (2016) Abelian floquet symmetry-protected topological phases in one dimension. Phys. Rev. B 94(12):125105.
19. Roy S, Sreejith GJ (2016) Disordered chern insulator with a two-step floquet drive. Phys. Rev. B 94(21):214203.
20. Roy R, Harper F (2017) Floquet topological phases with symmetry in all dimensions. Phys. Rev. B 95(19):195128.
21. Wilczek F (2012) Quantum time crystals. Phys. Rev. Lett. 109(16):160401.
22. Bruno P (2013) Impossibility of spontaneously rotating time crystals: A no-go theorem. Phys. Rev. Lett. 111(7):070402.
23. Watanabe H, Oshikawa M (2015) Absence of quantum time crystals. Phys. Rev. Lett. 114(25):251603.
24. von Keyserlingk CW, Khemani V, Sondhi SL (2016) Absolute stability and spatiotemporal long-range order in floquet systems. Phys. Rev. B 94(8):085112.
25. Else DV, Bauer B, Nayak C (2016) Floquet Time Crystals. Phys. Rev. Lett. 117(9):090402.
26. Else DV, Bauer B, Nayak C (2017) Prethermal phases of matter protected by time-translation symmetry. Phys. Rev. X 7(1):011026.
27. Yao NY, Potter AC, Potirniche ID, Vishwanath A (2017) Discrete time crystals: Rigidity, criticality, and realizations. Phys. Rev. Lett. 118(3):030401.
28. Khemani V, von Keyserlingk CW, Sondhi SL (2017) Defining time crystals via representation theory. Phys. Rev. B 96(11):115127.
29. Ho WW, Choi S, Lukin MD, Abanin DA (2017) Critical time crystals in dipolar systems. Phys. Rev. Lett. 119(1):010602.
30. Zhang J, et al. (2017) Observation of a discrete time crystal. Nature 543:217 EP –.
31. Choi S, et al. (2017) Observation of discrete time-crystalline order in a disordered dipolar many-body system. Nature 543:221 EP –.
32. Rovny J, Blum RL, Barrett SE (2018) ^{31}p nmr study of discrete time-crystalline signatures in an ordered crystal of ammonium dihydrogen phosphate.
33. Rovny J, Blum RL, Barrett SE (2018) Observation of discrete time-crystalline signatures in an ordered dipolar many-body system.
34. Huse DA, Nandkishore R, Oganesyan V, Pal A, Sondhi SL (2013) Localization-protected quantum order. Phys. Rev. B 88(1):014206.
35. Vosk R, Altman E (2014) Dynamical quantum phase transitions in random spin chains. Phys. Rev. Lett. 112(21):217204.
36. Pekker D, Refael G, Altman E, Demler E, Oganesyan V (2014) Hilbert-glass transition: New universality of temperature-tuned many-body dynamical quantum criticality. Phys. Rev. X 4(1):011052.
37. Ponte P, Chandran A, Papić Z, Abanin DA (2015) Periodically driven ergodic and many-body localized quantum systems. Annals of Physics 353:196 – 204.
38. Ponte P, Papić Z, Huveneers Fmc, Abanin DA (2015) Many-body localization in periodically driven systems. Phys. Rev. Lett. 114(14):140401.
39. Lazarides A, Das A, Moessner R (2015) Fate of many-body localization under periodic driving. Phys. Rev. Lett. 115(3):030402.
40. Abanin DA, Roeck WD, Huveneers F (2016) Theory of many-body localization in periodically driven systems. Annals of Physics 372:1 – 11.
41. De Roeck W, Huveneers Fmc (2017) Stability and instability towards delocalization in many-body localization systems. Phys. Rev. B 95(15):155129.
42. Luitz DJ, Huveneers Fmc, De Roeck W (2017) How a small quantum bath can thermalize long localized chains. Phys. Rev. Lett. 119(15):150602.
43. Ponte P, Laumann CR, Huse DA, Chandran A (2017) Thermal inclusions: how one spin can destroy a many-body localized phase. Philosophical Transactions of the Royal Society of London A: Mathematical, Physical and Engineering Sciences 375(2108).
44. Abanin DA, De Roeck W, Huveneers Fmc (2015) Exponentially slow heating in periodically driven many-body systems. Phys. Rev. Lett. 115(25):256803.
45. Kuwahara T, Mori T, Saito K (2016) Floquet–magnus theory and generic transient dynamics in periodically driven many-body quantum systems. Annals of Physics 367:96 – 124.
46. Fisher DS (1992) Random transverse field ising spin chains. Phys. Rev. Lett. 69(3):534–537.
47. Fisher DS (1994) Random antiferromagnetic quantum spin chains. Phys. Rev. B 50(6):3799–3821.
48. Fisher DS (1995) Critical behavior of random transverse-field ising spin chains. Phys. Rev. B 51(10):6411–6461.
49. Damle K, Huse DA (2002) Permutation-symmetric multicritical points in random antiferromagnetic spin chains. Phys. Rev. Lett. 89(27):277203.
50. Motrunich O, Mau SC, Huse DA, Fisher DS (2000) Infinite-randomness quantum ising critical fixed points. Phys. Rev. B 61(2):1160–1172.
51. Vosk R, Huse DA, Altman E (2015) Theory of the many-body localization transition in one-dimensional systems. Phys. Rev. X 5(3):031032.
52. Shirley JH (1965) Solution of the schrödinger equation with a hamiltonian periodic in time. Phys. Rev. 138(4B):B979–B987.
53. Sambe H (1973) Steady states and quasienergies of a quantum-mechanical system in an oscillating field. Phys. Rev. A 7(6):2203–2213.
54. Nandkishore R, Huse DA (2015) Many-body localization and thermalization in quantum statistical mechanics. Annual Review of Condensed Matter Physics 6(1):15–38.
55. Jiang L, et al. (2011) Majorana fermions in equilibrium and in driven cold-atom quantum wires. Phys. Rev. Lett. 106(22):220402.
56. (year?). See supplemental material.
57. Vasseur R, Potter AC, Parameswaran SA (2015) Quantum criticality of hot random spin chains. Phys. Rev. Lett. 114(21):217201.
58. Doty CA, Fisher DS (1992) Effects of quenched disorder on spin-1/2 quantum xxz chains. Phys. Rev. B 45(5):2167–2179.
59. Barghathi H, Hrahsheh F, Hoyos JA, Narayanan R, Vojta T (2015) Strong-randomness phenomena in quantum ashkin–teller models. Physica Scripta 2015(T165):014040.
60. Slagle K, You YZ, Xu C (2016) Disordered XYZ spin chain simulations using the spectrum bifurcation renormalization group. Phys. Rev. B 94(1):014205.
61. Monthus C (2017) Periodically driven random quantum spin chains: real-space renormalization for floquet localized phases. Journal of Statistical Mechanics: Theory and Experiment 2017(7):073301.
62. Refael G, Moore JE (2004) Entanglement entropy of random quantum critical points in one dimension. Phys. Rev. Lett. 93(26):260602.
63. Huang Y, Moore JE (2014) Excited-state entanglement and thermal mutual information in random spin chains. Phys. Rev. B 90(22):220202.
64. Bauer B, Nayak C (2013) Area laws in a many-body localized state and its implications for topological order. Journal of Statistical Mechanics: Theory and Experiment 2013(09):P09005.
65. Serbyn M, Papić Z, Abanin DA (2013) Local conservation laws and the structure of the many-body localized states. Phys. Rev. Lett. 111(12):127201.
66. Kim K, et al. (2010) Quantum simulation of frustrated ising spins with trapped ions. Nature 465:590 EP –.
67. Blatt R, Roos CF (2012) Quantum simulations with trapped ions. Nature Physics 8:277 EP –.
68. Smith J, et al. (2016) Many-body localization in a quantum simulator with programmable random disorder. Nature Physics 12:907 EP –.
69. Peschel I (2003) Calculation of reduced density matrices from correlation functions. J. Phys. A: Math. Gen. 36(14):L205.
70. Eisler V, Peschel I (2007) Evolution of entanglement after a local quench. J. Stat. Mech. 2007(06):P06005.
71. Towns J, et al. (2014) XSEDE: Accelerating Scientific Discovery. Computing in Science & Engineering 16(5):62–74.